fermentation

MDPI

Article

Mathematical Modeling of Nitrification in Mixed Cultures: Insights into Nitrite-Oxidizing Bacteria Growth and Ammonia Starvation Effect

Georgios Manthos [1,2], Leila Abbaszadeh [1,2], Dimitris Zagklis [1,2] and Michael Kornaros [1,2,*]

[1] Laboratory of Biochemical Engineering & Environmental Technology (LBEET), Department of Chemical Engineering, University of Patras, 26504 Patras, Greece; geomanthos@chemeng.upatras.gr (G.M.); chem.tec.v@gmail.com (L.A.); dimitriszag@chemeng.upatras.gr (D.Z.)
[2] Institute of Circular Economy and Environment (ICEE), University of Patras' Research and Development Center, 26504 Patras, Greece
* Correspondence: kornaros@chemeng.upatras.gr

Abstract: Nitrification, a crucial process in wastewater treatment, involves the conversion of ammonium nitrogen to nitrate nitrogen through the sequential activities of ammonia-oxidizing bacteria (AOB) and nitrite-oxidizing bacteria (NOB). In the present study, a comprehensive mathematical model was developed to describe the nitrification process in mixed cultures involving isolated NOB and starved AOB. The growth equation for NOB was divided into anabolism and catabolism, elucidating the key substrates driving their metabolic activities. Considering the ammonia starvation effect, a single cell-based model was developed to capture the mass transfer phenomena across the AOB cell membrane. This addition allowed for a more accurate representation of the biological dynamics during starvation conditions. The model's accuracy was tested using experimental data that was not used in the model calibration step. The prediction's coefficient of determination (R^2) was estimated at 0.9. By providing insights into the intricate mechanisms underlying nitrification, this model contributes to the advancement of sustainable wastewater treatment practices.

Keywords: nitrification; modeling; starvation; AOB; nitrite-oxidizing bacteria (NOB); ammonia accumulation

Citation: Manthos, G.; Abbaszadeh, L.; Zagklis, D.; Kornaros, M. Mathematical Modeling of Nitrification in Mixed Cultures: Insights into Nitrite-Oxidizing Bacteria Growth and Ammonia Starvation Effect. *Fermentation* **2023**, *9*, 681. https://doi.org/10.3390/fermentation9070681

Academic Editor: Ricardo Aguilar-López

Received: 27 June 2023
Revised: 17 July 2023
Accepted: 18 July 2023
Published: 20 July 2023

1. Introduction

Currently, humans are producing approximately 210 Tg of reactive nitrogen per year [1] and more than half of this waste is released into the environment without treatment. Reactive nitrogen is highly mobile and most of it dissipates into the environment and cascades through air, waters and ecosystems [2]. Excess reactive nitrogen not only has a negative impact on human health, but also contributes to air and water pollution, and can lead to complex ecosystems collapsing. Nitrogen is usually present in wastewater in three forms (1) organic nitrogen compounds, (2) ammonium (NH_4^+) or ammonia (NH_3), depending on the pH, and (3) trace amounts of nitrite (NO_2^-) and nitrate (NO_3^-). However, organic fractions such as proteins, amino acids, and amino sugars are quickly degraded to ammonium either in the sewer systems or in the wastewater treatment tanks [3].

The most common method of removing nitrogen from wastewater is biological nitrogen removal (BNR) comprising of nitrification and denitrification, which is considered economical and efficient. In conventional BNR plants, ammonia, which was suggested to be the true substrate for the oxidation process and not ammonium [4], is oxidized to nitrate via autotrophic nitrification followed by its reduction to nitrogen gas via heterotrophic denitrification. Nitrification, the biological oxidation of ammonium to nitrite and nitrate, is essential in nitrogen cycling in wastewater treatment reactors. Groups of organisms known to be involved in this process include autotrophic ammonia-oxidizing bacteria (AOB), and nitrite-oxidizing bacteria (NOB) [5].

AOB are present in most natural aerobic environments, including soils, freshwater, and marine ecosystems [6–8] and some low-oxygen environments and subsurface sediments [9]. AOB cultures are also dominant in many ammonium-rich environments that have been impacted by anthropogenic nitrogen sources such as fertilizers, wastewater, and industrial by-products [7]. Despite its abundance, it is sometimes exposed to stress caused by low substrate concentrations and even its absence.

The starvation behavior of several AOB belonging to different phylogenetic groups has previously been investigated. Nitrogen removal efficiency in an anammox-partial nitrification reactor reached 95% when subjected to repeated starvation and reactivation periods [10]. Laboratory observations can clearly show different strategies of AOB according to N source levels in oligotrophic or N-rich environments [11]. During nitrification, the oxidation of ammonia by AOB is the most decisive process rate, which is catalyzed by two types of enzymes, ammonia monooxygenase (AMO), which leads to hydroxylamine (NH_2OH) as an intermediate, and hydroxylamine reductase (HAO), which oxidizes NH_2OH to nitrite [12]. Starvation stress can affect the level of both enzymes [13]. The effect of short-term ammonia starvation on non-starving cultures of *N. briensis* shows potential ammonia-oxidizing activities of 200 to 250 μM N h^{-1}, and this activity decreased only slowly during starvation up to 10 days. Within 10 min after the addition of fresh NH_4^+-N, 100% of activity was regained. Starvation negatively affected AMO mRNA levels, while during recovery, an increase in amoA mRNA expression was detected simultaneously [14]. In a similar study that was conducted with the enriched culture of freshwater ammonia oxidizers (AOB-G5-7), 16S rRNA and HAO were maintained during starvation, and AMO and mRNA were affected by starvation for 50 days [15].

Nitrosomonas europaea related to *Nitrosomonas* cluster 7 (a group of AOB that has been identified in environments such as wastewater, which contain high concentrations of NH_4^+) was rapidly reactivated after periods of starvation, in the presence of ammonium by batch and retentostat experiments [11,16,17]. Moreover, the *Nitrosomonas cryotolerans* species (marine AOB) have shown a similarly rapid response to the presence of ammonia [18–20]. On the other hand, members of *Nitrosomonas* cluster 6a (*Nitrosomonas oligotrophic* group) are often found in freshwater environments [21–23]. One of these species (*Nitrosospira briensis*), often found in terrestrial habitats, regain their activity slower than *Nitrosomonas europaea* after long-term starvation of 10 weeks or 4 months [11,16]. Experiments conducted in the enriched medium containing *Nitrosomonas eutropha* in CSTR reactors under different steady-state substrate concentrations showed intracellular ammonium concentrations from six different reactors. Intracellular total ammonium nitrogen (TAN) accumulations, gradually increased from a basal value of ~1 M to much higher values (grown under an oligotrophic environment) [4]. In experiments about the physiology of nitrifiers and stress response to optimize the removal of nutrients and design advanced processes, ammonium deprivation for 3 days resulted in fast ammonium/ammonia accumulation upon nitrogen availability, with a maximum uptake rate of 3.87 mmol gprotein^{-1} min^{-1}. Furthermore, a delay in the production of nitrate was observed with increasing starvation periods, resulting in slower recovery and a lower nitrification rate compared to non-starved cells. The maximum accumulation capacity observed was 8.51% (*w/w*) independently of the external nitrogen concentration, at a range of 250–750 mg N L^{-1}, while pH significantly affected ammonia oxidizers' response, with alkaline values enhancing nitrogen uptake [24].

This work aimed to develop a holistic mathematical model that can describe the nitrification process in different substrate concentrations, pH, and starvation conditions. Several authors have developed kinetic models for nitrate production from activated sludge. The main equation that describes microbial growth is the Monod model. Several parameters affect the production rate of biomass, some of them are the temperature, the pH value, and the hydraulic retention time [25]. Other authors developed more fundamental models breaking the ammonium oxidation process into two enzymatic sub-processes (ammonia monooxygenase reaction and hydroxylamine oxidoreductase reaction) with different maximum specific growth rates [26]. Using the proposed model to accurately predict the

nitrification process performance can assist nitrification design applications in wastewater treatment facilities and optimizing the operating conditions for the environmental and economic feasibility of full-scale BNR plants.

2. Materials and Methods

2.1. Isolation and Enrichment of Nitrifying Microorganisms

In this study, two kinds of enriched ammonia-oxidizing bacteria (AOB) and purified nitrite-oxidizing bacteria (NOB) were evaluated. The initial sludge consortium was originated from the aeration tank of the biological wastewater treatment plant of the University of Patras (Rio, Patras, Greece). The synthetic growth medium used for the enrichment of nitrifying microorganisms included 0.956 g L^{-1} ammonium chloride (NH_4Cl) as a nitrogen source for AOB and 1.232 g L^{-1} sodium nitrite ($NaNO_2$) for NOB. In addition, 10.52 g L^{-1} potassium hydrogen phosphate (K_2HPO_4) and 4.72 g L^{-1} potassium dihydrogen phosphate (KH_2PO_4) were used both to maintain the pH value in the range of 7.3–7.4 and to provide a phosphorus source to the sludge. A quantity of 3.52 g L^{-1} of sodium hydrogen carbonate ($NaHCO_3$) was added in excess, to ensure that the nitrification process was not limited by alkalinity. Finally, 1 mL L^{-1} trace elements, including 1 g L^{-1} $FeSO_4 \cdot 7H_2O$, 1 g L^{-1} $MgSO_4 \cdot 7H_2O$, 0.25 g L^{-1} $CaCl_2 \cdot 2H_2O$, 0.25 g L^{-1} $Na_2MoO_4 \cdot 2H_2O$, 0.1 g L^{-1} H_3BO_3, and 5 mL L^{-1} H_2SO_4 were added to the medium [24]. During the isolation process which followed, 50 mL of the initial amount of active sludge was mixed with 450 mL of synthetic growth medium in a Duran flask (Schott). The flask was incubated in a stirred water bath, at 25 °C and 100 rpm. To ensure aerobic conditions, air was provided using a ventilation pump under a constant flow rate of 2 L min^{-1}. After the complete oxidation of ammonia to nitrate, biomass was collected through centrifugation and was inoculated in a fresh growth medium.

Enriched activated sludge was used as an initial consortium in order to isolate NOB. The resulting enriched liquid culture was inoculated onto Petri dishes containing curdled growth medium, using agar. The whole isolation process was performed under sterile conditions using a laboratory sterile laminar flow chamber. The inoculated plates were placed in an incubator (BMT Incucell V) at 25 °C for 3 to 4 weeks. Several recultures were performed using the observed colonies in order to purify the bacteria culture, on a solid medium. Following this step, isolated cells were transferred to liquid cultures containing $NaNO_2$ as substrate.

Fifteen different microbial cultures were prepared to examine the nitrification effect and to develop a general mathematical model. More specifically, mixed bacterial cultures with both NOB and AOB were cultivated and monitored in four different pH values (6.5–8 with a step of 0.5) for an initial ammonium nitrogen concentration of 100 mg L^{-1} and 250 mg L^{-1}. Moreover, three different experiments with mixed culture in different initial ammonium nitrogen concentrations (100 mg L^{-1}, and 700 mg L^{-1}) with a pH value of 7.8 were used for model calibration. Regarding the starvation experiments, the enriched nitrifying bacterial culture was cultivated in a nitrogen-depleted medium for 1, 2, 3, 4, and 5 days, respectively, and was subsequently exposed to 250 mg NH_4^+-N L^{-1} in four different pH conditions (6.5 to 8 with a step of 0.5). The pH value was monitored daily with an electronic pH meter (Thermo Scientific, Orion ROSS Ultra Refillable Ph/ATC Triode) and was adjusted manually to the pre-set value, when it was needed. Finally, pure NOB cultures with nitrite ions (from sodium nitrite) in a concentration of 100 mg L^{-1} and both nitrite and ammonium nitrogen (1 mg L^{-1}) as substrate were used to evaluate the kinetic parameters in the different metabolic pathways of the NOB culture. All experiments were performed in duplicate.

2.2. Analytical Techniques

Regarding the nitrification process evaluation, nitrite (NO_2^-) and nitrate (NO_3^-) ions were determined by ion chromatography (DIONEX ICS-3000) equipped with a Dionex IonPac^{TM} AS19 (4 × 250 mm) and a DIONEX conductivity detector. The column tempera-

ture was set at 30 °C and detector temperature at 35 °C. The mobile phase used consisted of purified water and HCl 3 M. The flow rate was set at 0.8 mL min^{-1} while the run-time analysis was 30 min. Initially, the eluent was 100% purified water maintained for 18 min. The concentration of HCl 3 M was increased from 15% to 50% for 3 min (18–21 min of the method) and maintained for 4 min (21–25 min of the method). Then, the same eluent was reduced from 50% to 15% for 0.5 min (25–25.5 min of the method). Finally, the concentration of HCl 3 M was slightly increased from 15% to 18% for 4.5 min (25.5–30 min of the method). Ammonium nitrogen was measured based on the Phenate method [27]. Biomass concentration was measured as dry cell weight (DW), according to a modified method of *Standard Methods* (Method 2540) for an estimation of Total Suspended Solids (TSS), using GF/F grade filters [28]. All analytical measurements were performed in duplicate.

2.3. Model Development

The proposed model was based on the well-established model ASM1 which describes the biological wastewater treatment process [29]. This model describes the mass balances among the different forms of nitrogen in the nitrification process (ammonium to nitrate, nitrite to nitrate). Different microorganisms' species were involved in these steps. AOB were involved in the nitrite formation from ammonium nitrogen and NOB were involved in the nitrate formation. Regarding the NOB metabolic pathway, the microbial process was divided into anabolism and catabolism. During anabolism, the NOB cells utilize ammonium nitrogen as the nitrogen source to form new biomass cells. If there is a lack of ammonium nitrogen in the medium, an intracellular conversion of nitrite to ammonium is carried out to cover the microorganism's nitrogen demands. Regarding the energy demands of NOB culture (catabolism), only nitrite is consumed to form nitrate in the medium. A brief description of the major processes included in the proposed model are presented schematically in Figure 1a.

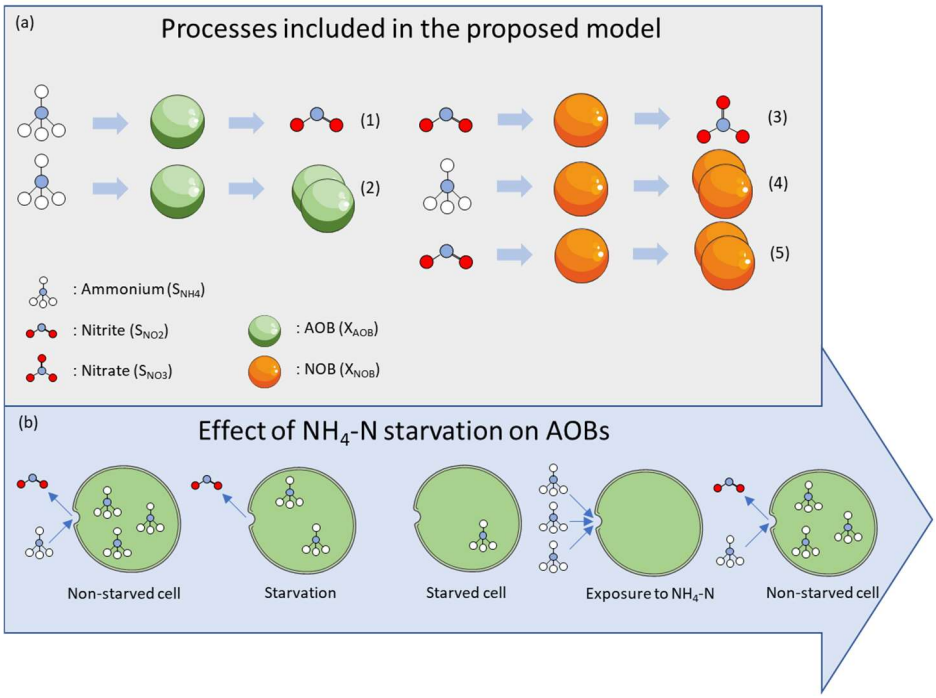

Figure 1. Processes included in the proposed model: conversion of NH_4^+ to NO_2^- by AOB (1), assimilation of NH_4-N in AOB biomass for new cell formation (2), conversion of NO_2^- to NO_3^- by NOB (3), assimilation of NH_4-N in NOB biomass for new cell formation (4), assimilation of NO_2-N in NOB biomass for new cell formation (5) (**a**). Effects of NH_4-N starvation on the accumulation of NH_4^+ inside AOB cells (**b**).

As presented in Figure 1, the ammonium nitrogen (S_{NH4}) of the medium in a mixed AOB-NOB culture is consumed either for AOB (X_{AOB}) (anabolism and catabolism) or NOB anabolism (X_{NOB}). The separation of anabolism and catabolism in AOB growth is expressed mathematically from the parameters $i_{x,b,}$ and Y_{AOB} in Equations (8) and (9), where $i_{x,b}$ represents the fraction of nitrogen in biomass (measured value 3.87 $g_N/g_{biomass}$) and Y_{AOB} denotes the AOB yield [$g_{biomass}/g_N$]. Regarding the growth rates of both AOB and NOB, the widely used Monod equation was implemented in the proposed model. The maximum specific growth rate for each microbial group is presented as μ_{max}.

Regarding the anabolism/catabolism separation in the NOB culture, a new term was implemented in the biomass equation to switch the biomass maximum specific growth rate with the presence or absence of ammonium in the medium. Alongside the new term, a parameter was implemented in the mass balance (K_{NH4}). When the concentration of the ammonium nitrogen (S_{NH4}) in the medium was much greater than the K_{NH4} parameter, the NOB biomass growth rate was ruled from the $\mu_{max,1}$ specific growth rate. On the other hand, when the ammonium nitrogen value was less than K_{NH4}, the biomass growth was determined from the $\mu_{max2,NO2}$. Moreover, a decrease in NOB biomass growth rate was observed when the concentration of ammonium nitrogen in the medium was high. This effect was described with the implementation of the well-established term of Andrews kinetics (i.e., substrate inhibition) for ammonium nitrogen [30].

Regarding the experimental results for the nitrate formation, non-proportional nitrate production was observed compared to the corresponding biomass growth. Hence, a nitrate production rate parameter (q_{max}) was implemented in the model. This parameter was set as an independent parameter concerning biomass's maximum specific growth rate. Moreover, a difference in the nitrate production rate was observed with the presence or absence of ammonium quantities in the pure NOB cultures. In order to express this difference, the maximum nitrate production rate was divided into two different parameters ($q_{max,1}$, $q_{max,2}$) depending on the concentration of ammonium nitrogen in the culture. Besides the inhibition in NOB biomass growth with the excess of ammonium nitrogen in the medium, no inhibition phenomena were observed in nitrate formation when the $q_{max,2}$ determined the nitrate production. For this reason, no implementation of Andrews's term was considered in this mass balance equation.

Regarding the pH inhibition effects, multiple phenomena and assumptions were considered. A partial inhibition in ammonium consumption by AOB was observed in the low pH values. This inhibition was expressed in the model with I_{AOB} term by a sigmoid function (Equation (1)) [31]:

$$I_{AOB} = \frac{1}{1 + \exp(A(K - pH))} \quad (1)$$

where A denotes a fitting parameter and K represents the half-saturation constant for the pH. Regarding the high pH values, an inhibition of free ammonia was considered in the proposed model. The ammonia–ammonium equilibrium was used to estimate the ammonia nitrogen concentration from ammonium concentration (ammonium nitrogen and ammonia nitrogen) in the present pH values (Equation (2))

$$S_{NH3} = S_{NH4} \frac{K_\alpha}{10^{-pK_\alpha} + 10^{-pH}} \quad (2)$$

where K_α represents the equilibrium constant of ammonia–ammonium equilibrium (value 5.6×10^{-10}).

The estimated ammonia concentration was implemented in I_{NOB} inhibition terms involved in biomass growth and nitrate formation. One extra parameter (K_{NH3}) was used to quantify the ammonia inhibition in the two mass balances. The final inhibition terms are presented in Equation (3):

$$I_{NOB} = \frac{K_{NH3}}{K_{NH3} + S_{NH3}} \quad (3)$$

Finally, regarding the modeling of the starvation effect [24], a single cell-based model was used according to Figure 1b. It was assumed that the amount of stored nitrogen inside the cell (X_{Nst}) was in equilibrium with the ammonium nitrogen in the medium, through the semipermanent cell membrane. The equilibrium was carried out with the osmotic pressure on the two sides of the membrane as the driving force. For the calculations, the percentage of moisture inside the cell was set as 70% *w/w* according to [32], and the equilibrium constant k_D [g_N $g_{N\text{-}NH4}{}^{-1}$]. The rate of equilibrium was determined by the k_N parameter and the mass flux. The pH value of the medium affects the starvation effect according to previous experimental work [24]. For this reason, Equation (1) was implemented in the mass balance of internally stored nitrogen in order to inhibit the overall phenomenon at low pH values. The final model equations are summarized in Equations (4)–(11).

$$\frac{dx_{AOB}}{dt} = \mu_{max,NH4}\frac{S_{NH4}}{S_{NH4}+K_{S,NH4}}x_{AOB}I_{AOB} \tag{4}$$

$$\frac{dx_{NOB,NO2}}{dt} = \mu_{max1,NO2}\frac{S_{NO2}}{S_{NO2}+K_{S,NO2}}\frac{K_{NH4}}{S_{NH4}+K_{NH4}}x_{NOB} \tag{5}$$

$$\frac{dx_{NOB,NH4}}{dt} = \mu_{max2,NO2}\frac{S_{NO2}}{S_{NO2}+K_{S,NO2}}\frac{S_{NH4}}{S_{NH4}+K_{S,NH4}+\frac{S_{NH4}^2}{K_{SS,NH4}}}x_{NOB}I_{NOB} \tag{6}$$

$$\frac{dx_{NOB}}{dt} = \frac{dx_{NOB,NO2}}{dt}+\frac{dx_{NOB,NH4}}{dt} \tag{7}$$

$$\frac{dS_{NH4}}{dt} = -\left(i_{xb}+\frac{1}{Y_{AOB}}\right)\frac{dx_{AOB}}{dt}-i_{xb}\frac{dx_{NOB,NH4}}{dt}-\frac{dX_{Nst}}{dt} \tag{8}$$

$$\frac{dS_{NO2}}{dt} = \frac{1}{Y_{AOB}}\frac{dx_{AOB}}{dt}-i_{xb}\frac{dx_{NOB,NO2}}{dt}-\frac{dS_{NO3}}{dt} \tag{9}$$

$$\begin{aligned}\frac{dS_{NO3}}{dt} &= q_{max,1}\frac{S_{NO2}}{S_{NO2}+K_{S,NO2}}\frac{K_{NH4}}{S_{NH4}+K_{NH4}}x_{NOB}I_{NOB}\\ &+ q_{max,2}\frac{S_{NO2}}{S_{NO2}+K_{S,NO2}}\frac{S_{NH4}}{S_{NH4}+K_{S,NH4}}x_{NOB}\end{aligned} \tag{10}$$

$$\frac{dX_{Nst}}{dt} = -k_N\left(k_D S_{NH4}\frac{moist_{biomass}}{1-moist_{biomass}}x_{AOB}-X_{Nst}\right)I_{AOB} \tag{11}$$

2.4. Numerical Methods

Different sets of experimental data were used to train and calibrate the proposed model. In the calibration step, experimental data from both pure NOB and mixed AOB-NOB cultures in different pH and starvation conditions were used. Initial parameters' values were set to start the numerical solution for minimizing the objective function of the sum of the squares of errors normalized with the experimental value (relative error) [33] (Equation (12)):

$$\min_x \sum_{i=1}^{n}\left(\frac{y_{exp,i}-y_{sim,i}}{y_{exp,i}}\right)^2 \tag{12}$$

where x denotes the vector of the optimized parameters, $y_{exp,i}$ represents the experimental value in point i, $y_{sim,i}$ represents the theoretical value in point i, and n denotes the length of the experimental point vector.

The optimization algorithm was developed in MATLAB R2018a software, a computing platform used by many engineers and scientists for data analysis and model optimization. The native function *fmincon* was used as a nonlinear programming solver using 'interior-point' as an algorithm, where the *fmincon* sets components of initial values that are equal to the interior of the bound region.

Because of the large number of the parameter vector, certain 'sub-runs' were performed with only the key parameters to be estimated, as explained in the results section. The final model training step included the overall optimization and parameter estimation in a narrow range above and below the final parameter value. Certain experimental data were excluded from the model training step to be used in model validation and testing. The estimated parameters were kept as constants in the model validation process aiming to predict the system behavior for experiments inside the range of the conditions used for optimizing the model parameters.

3. Results

3.1. Determination of Kinetic Parameters—Non-Starved Cultures

The simulated results with the experimental data used for model calibration are presented in Figure 2. Biomass growth, and nitrite and nitrate formation, were observed in the investigated pH range from 7 to 8. A strong inhibition was exhibited in the experiment with a pH value of 6.5 (Figure 2c), where no biomass growth or product formation was observed. The maximum nitrate formation was exhibited when the initial concentration of ammonium nitrogen was 700 mg L^{-1} (Figure 2b), with the maximum nitrate concentration for both the model and experimental results being 800 mg L^{-1}. Regarding the nitrite concentration, almost-zero values were observed for low pH values and initial ammonium nitrogen concentrations. This behavior differs for the high initial ammonium nitrogen concentration (250 mg L^{-1}), with pH values equal to 7 and 8 (Figure 2f,h). A nitrite–nitrogen concentration of 50 mg L^{-1} was exhibited with a rapid consumption rate for a pH value equal to 7 (complete nitrate consumption at 0.5 d). The partial inhibition of this rate was exhibited in a pH value equal to 8, where the nitrite nitrogen elimination was observed at day 5 (Figure 2h). A good fit of model calibration results to experimental data was exhibited (R^2 = 0.7), considering that the proposed model structure describes all process boundaries and limitations for all the investigated parameters (bulk pH value, initial concentration of ammonium and nitrite nitrogen, culture qualitative and quantitative characteristics).

Regarding the isolated NOB kinetics, two different experiments (with and without ammonium–nitrogen addition) were conducted (Figure 3) in order to evaluate the different kinetic parameters for anabolism and catabolism. A slow biomass production rate was observed for both experiments (with and without ammonia) compared to the results that were exhibited in the literature [29,34].

The estimated parameter values are presented in Table 1. The rates for biomass growth and product formation for the NOB were observed significantly higher than the rates concerning AOB (by 50%). This observation has also been reported in other studies. In the work of Liu et al. [35] three different mathematical models were used in order to evaluate the nitrification process. The maximum specific growth for both NOB and AOB was estimated in the same order of magnitude as the results of this study. In another study by Cui et al. [36] the biomass growth rate was estimated as significantly higher comparing the present work (1.95 d^{-1} compared with 0.1 d^{-1}). This fact may be attributed to the higher culture temperature (35 °C) compared to the culture temperature of this work. The same order of magnitude of μ_{max} values was obtained in the work of Thalla et al. [37], even if the parameter estimation was performed using linear regression.

3.2. Determination of Kinetic Parameters—Starved Cultures

Based on the proposed analysis, during the model calibration, the ammonium starvation effect on AOB was examined (Figure 4). The starvation effect was observed during the first day of cultivation (during the first 4 h). The proposed model successfully simulated this effect with the estimation of the parameters of k_N and k_D. The process rate was determined by the parameter k_N with a value equal to 25 d^{-1}, two orders of magnitude higher than the other biological rates. Since the starvation effect affects only the AOB, the pH inhibition was determined through common parameters for the starvation effect and AOB biomass growth. However, when the pH is below neutral or mild alkaline levels, the

amount of free ammonia typically decreases. This leads to a decrease in growth, substrate consumption, and enzyme function, as discussed in previous works [24,38].

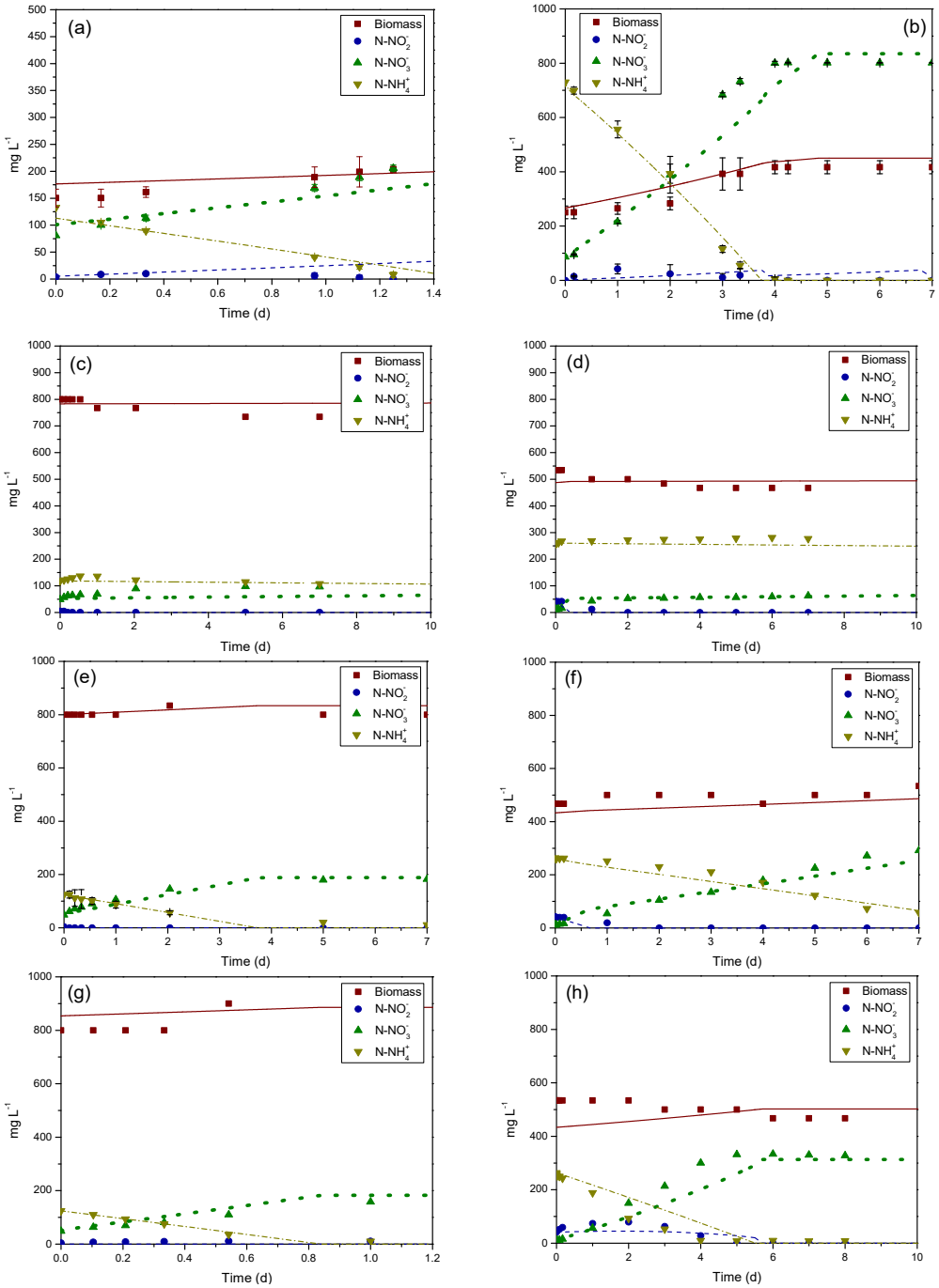

Figure 2. Experimental data and model results (continuous and dotted lines) for nitrification at pH 7.8, mixed cultures (NOB and AOB) and initial ammonium–nitrogen concentration of 100 mg L^{-1} (**a**), initial ammonium–nitrogen concentration 700 mg L^{-1} (**b**), pH 6.5 and initial ammonium–nitrogen concentration of 100 mg L^{-1} (**c**), pH 6.5 and initial ammonium–nitrogen concentration of 250 mg L^{-1} (**d**), pH 7 and initial ammonium–nitrogen concentration of 100 mg L^{-1} (**e**), pH 7 and initial ammonium–nitrogen concentration of 250 mg L^{-1} (**f**), pH 8 and initial ammonium–nitrogen concentration of 100 mg L^{-1} (**g**), and pH 8 and initial ammonium–nitrogen concentration of 250 mg L^{-1} (**h**).

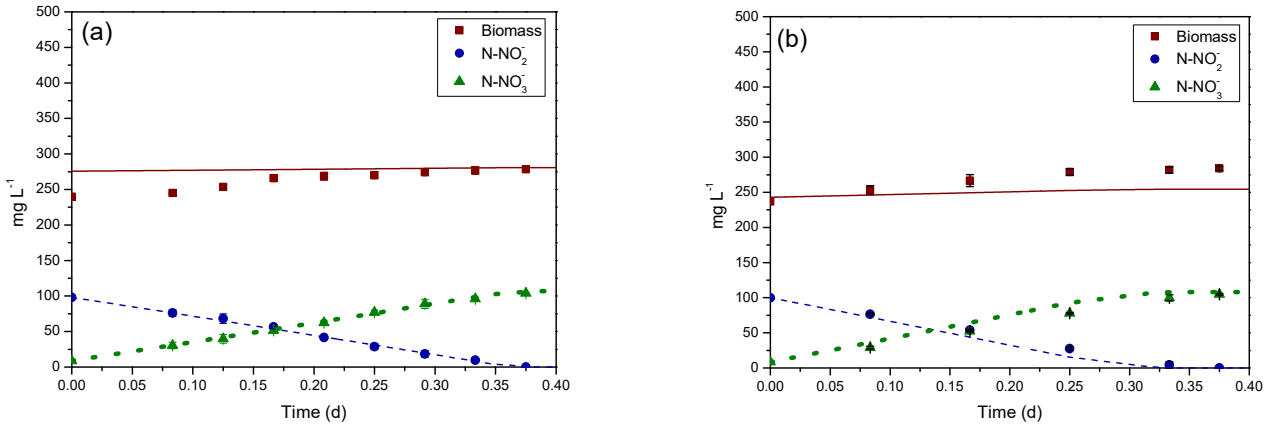

Figure 3. Experimental data and model results (continuous and dotted lines) for nitrification at pH 7.8 of NOB isolated culture with ammonium and nitrite nitrogen as substrate (**a**), and nitrite nitrogen as substrate (**b**).

Table 1. Estimated parameter values for the proposed nitrification model, optimized with the experimental data sets with different pH values, initial substrate concentration, different microorganisms, and starved and non-starved bacteria.

Parameter	Value	Units
$\mu_{max1,NO2}$	0.158	d^{-1}
$\mu_{max2,NO2}$	0.083	d^{-1}
$\mu_{max,NH4}$	0.091	d^{-1}
$q_{max,1}$	1.365	$g_{N\text{-}NO3}\ g_{biomass}^{-1}\ d$
$q_{max,2}$	0.788	$g_{N\text{-}NO3}\ g_{biomass}^{-1}\ d$
$K_{S,NO2}$	0.003	$g_{N\text{-}NO2}\ L^{-1}$
$K_{S,NH4}$	0.002	$g_{N\text{-}NH4}\ L^{-1}$
Y_{AOB}	0.141	$g_{biomass}\ g_{N\text{-}NH4}^{-1}$
K_{NH4}	4×10^{-4}	$g_{N\text{-}NH4}\ L^{-1}$
$K_{SS,NH4}$	7.555	$g_{N\text{-}NH4}\ L^{-1}$
A	6.758	-
K	7.713	-
K_{NH3}	7.819	$g_{N\text{-}NH3}\ L^{-1}$
k_N	25.07	d^{-1}
k_D	0.099	$g_N\ g_{N\text{-}NH4}^{-1}$

3.3. Model Validation

Based on the proposed analysis, it was deemed necessary to assess the model's accuracy using experimental data that was not used in the model calibration step. Two experiments with intermediate pH conditions (pH value 7.5) were used for this purpose. The main difference between these experiments was the initial concentration of ammonium–nitrogen in the bulk (100 mg L^{-1} and 250 mg L^{-1}, respectively). The results of the model prediction are presented in Figure 5. The maximum concentration of nitrate nitrogen reached the value of 200 mg L^{-1} and 350 mg L^{-1} (obviously as result of the non-starved AOB cells used in this run) for both the experimental data and theoretical simulations in the experiment, with initial ammonium nitrogen concentrations of 100 mg L^{-1} and 250 mg L^{-1}, respectively. The model's prediction R^2 was estimated at 0.9, indicating the high model's accuracy.

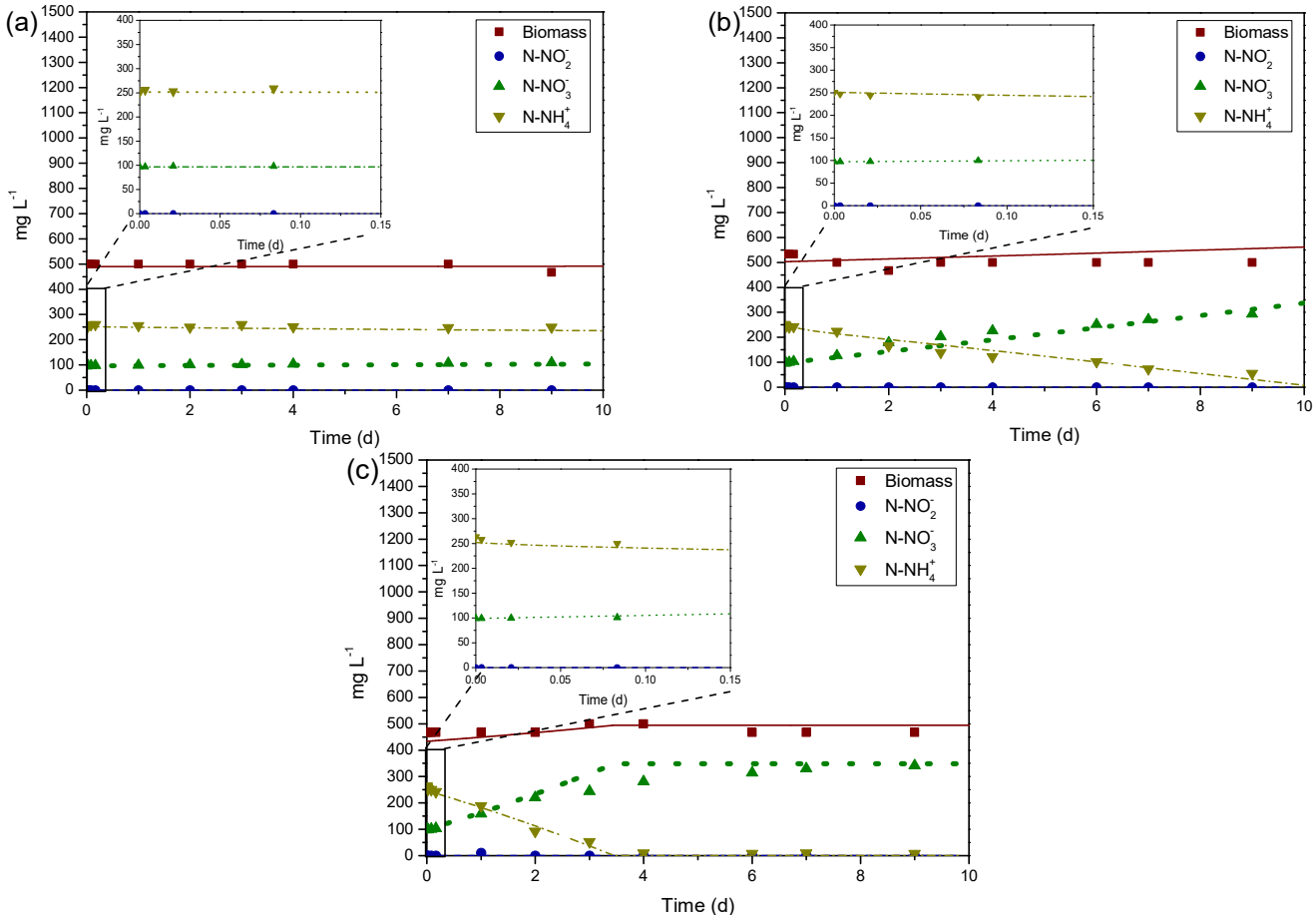

Figure 4. Experimental data and model results (continuous and dotted lines) for the nitrification of starved bacteria at (**a**) pH 6.5, (**b**) pH 7, and (**c**) pH 8.

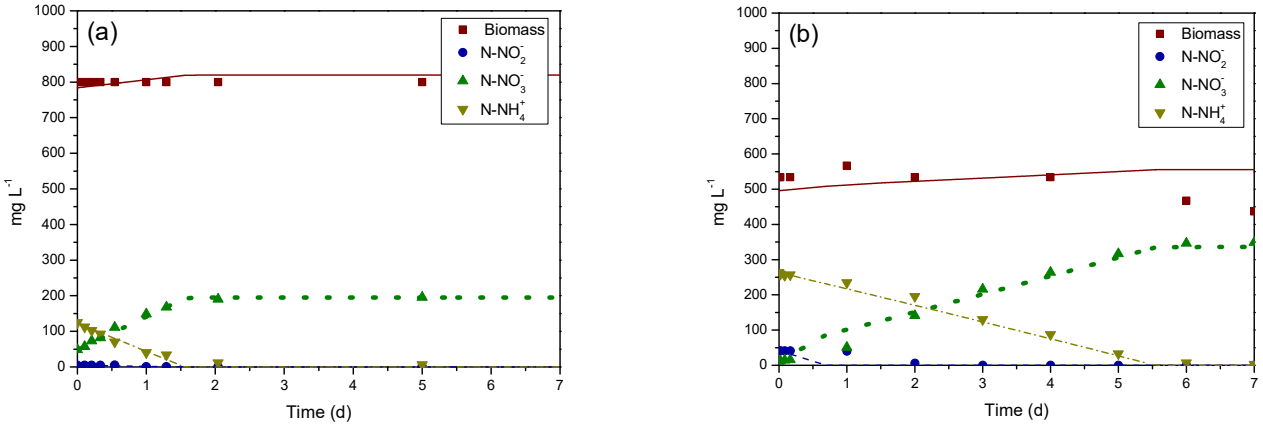

Figure 5. Experimental data and model prediction for nitrification process for mixed culture at pH 7.5 with ammonium nitrogen initial concentration 100 mg L^{-1} (**a**), and 250 mg L^{-1} (**b**).

4. Conclusions

A mathematical model describing the nitrification in mixed AOB-NOB, isolated NOB and mixed ammonium-N-starved AOB-NOB cultures was developed. Regarding the NOB growth equation, the biological process was divided into anabolism and catabolism. The analysis exhibits that ammonium nitrogen is the main nitrogen substrate of anabolism for NOB and nitrite–nitrogen is the secondary substrate that was assimilated by NOB if there is a lack of ammonium nitrogen in the bulk. Regarding the ammonium starvation

effect, a new variable (X_{Nst}) and two parameters (k_D and k_N) were implemented in the model to describe the mass transfer through the cell membrane of the AOB. The model could accurately predict microbial growth and product formation in different experiment conditions (pH, initial substrate concentration, microbial consortium) with $R^2 > 0.9$. The proposed model can be useful in the field of wastewater treatment and can be implemented as a tool for process optimization and decision making in full-scale treatment units.

Author Contributions: Conceptualization, G.M.; methodology, G.M.; software, G.M. and D.Z.; validation, G.M., D.Z. and L.A.; formal analysis, G.M. and L.A.; investigation, G.M., L.A. and D.Z.; resources, M.K.; data curation, G.M.; writing—original draft preparation, G.M. and L.A.; writing—review and editing, D.Z.; visualization, G.M.; supervision, M.K.; project administration, M.K. All authors have read and agreed to the published version of the manuscript.

Funding: This research received no external funding.

Institutional Review Board Statement: Not applicable.

Informed Consent Statement: Not applicable.

Data Availability Statement: Available upon request.

Conflicts of Interest: The authors declare no conflict of interest.

References

1. Holmes, D.E.; Dang, Y.; Smith, J.A. Nitrogen Cycling during Wastewater Treatment. *Adv. Appl. Microbiol.* **2019**, *106*, 113–192.
2. Erisman, J.W.; Galloway, J.N.; Seitzinger, S.; Bleeker, A.; Dise, N.B.; Petrescu, A.M.R.; Leach, A.M.; de Vries, W. Consequences of Human Modification of the Global Nitrogen Cycle. *Philos. Trans. R. Soc. B Biol. Sci.* **2013**, *368*, 20130116. [CrossRef]
3. Law, Y.; Ye, L.; Pan, Y.; Yuan, Z. Nitrous Oxide Emissions from Wastewater Treatment Processes. *Philos. Trans. R. Soc. B Biol. Sci.* **2012**, *367*, 1265–1277. [CrossRef]
4. Keerio, H.A.; Bae, W.; Park, J.; Kim, M. Substrate Uptake, Loss, and Reserve in Ammonia-Oxidizing Bacteria (AOB) under Different Substrate Availabilities. *Process Biochem.* **2020**, *91*, 303–310. [CrossRef]
5. Yao, Q.; Peng, D.-C. Nitrite Oxidizing Bacteria (NOB) Dominating in Nitrifying Community in Full-Scale Biological Nutrient Removal Wastewater Treatment Plants. *AMB Express* **2017**, *7*, 25. [CrossRef]
6. Hayden, C.J.; Beman, J.M. High Abundances of Potentially Active Ammonia-Oxidizing Bacteria and Archaea in Oligotrophic, High-Altitude Lakes of the Sierra Nevada, California, USA. *PLoS ONE* **2014**, *9*, e111560. [CrossRef]
7. Kowalchuk, G.A.; Stephen, J.R. Ammonia-oxidizing bacteria: A Model for Molecular Microbial Ecology. *Annu. Rev. Microbiol.* **2001**, *55*, 485–529. [CrossRef]
8. Mullan, G.D.O.; Ward, B.B. Relationship of Temporal and Spatial Variabilities of Ammonia-Oxidizing Bacteria to Nitrification Rates in Monterey Bay, California. *Appl. Environ. Microbiol.* **2005**, *71*, 697–705. [CrossRef]
9. Cao, H.; Hong, Y.; Li, M.; Gu, J.; Cao, H.; Hong, Y.; Li, M.; Gu, J. Lower Abundance of Ammonia-Oxidizing Archaea than Ammonia-Oxidizing Bacteria Detected in the Subsurface Sediments of the Northern South China Sea. *Geomicrobiol. J.* **2012**, *29*, 332–339. [CrossRef]
10. Pedrouso, A.; Tocco, G.; Val del Río, A.; Carucci, A.; Morales, N.; Campos, J.L.; Milia, S.; Mosquera-Corral, A. Digested Blackwater Treatment in a Partial Nitritation-Anammox Reactor under Repeated Starvation and Reactivation Periods. *J. Clean. Prod.* **2020**, *244*, 118733. [CrossRef]
11. Bollmann, A.; Bär-Gilissen, M.J.; Laanbroek, H.J. Growth at Low Ammonium Concentrations and Starvation Response as Potential Factors Involved in Niche Differentiation among Ammonia-Oxidizing Bacteria. *Appl. Environ. Microbiol.* **2002**, *68*, 4751–4757. [CrossRef]
12. Soliman, M.; Eldyasti, A. Ammonia-Oxidizing Bacteria (AOB): Opportunities and Applications—A Review. *Rev. Environ. Sci. Biotechnol.* **2018**, *17*, 285–321. [CrossRef]
13. Geets, J.; Boon, N.; Verstraete, W. Strategies of Aerobic Ammonia-Oxidizing Bacteria for Coping with Nutrient and Oxygen Fluctuations. *FEMS Microbiol. Ecol.* **2006**, *58*, 1–13. [CrossRef]
14. Bollmann, A.; Schmidt, I.; Saunders, A.M.; Nicolaisen, M.H. Influence of Starvation on Potential Ammonia-Oxidizing Activity and AmoA MRNA Levels of Nitrosospira Briensis. *Appl. Environ. Microbiol.* **2005**, *71*, 1276–1282. [CrossRef] [PubMed]
15. French, E.; Bollmann, A. Freshwater Ammonia-Oxidizing Archaea Retain AmoA MRNA and 16S RRNA during Ammonia Starvation. *Life* **2015**, *5*, 1396–1404. [CrossRef]
16. Laanbroek, H.J.; Bär-Gilissen, M.J. Weakened Activity of Starved Ammonia-Oxidizing Bacteria by the Presence of Pre-Activated Nitrobacter Winogradskyi. *Microbes Environ.* **2002**, *17*, 122–127. [CrossRef]
17. Tappe, W.; Laverman, A.; Bohland, M.; Braster, M.; Rittershaus, S.; Groeneweg, J.; Van Verseveld, H.W. Maintenance Energy Demand and Starvation Recovery Dynamics of Nitrosomonas Europaea and Nitrobacter Winogradskyi Cultivated in a Retentostat with Complete Biomass Retention. *Appl. Environ. Microbiol.* **1999**, *65*, 2471–2477. [CrossRef]

18. Jones, R.D.; Morita, R.Y. Survival of a Marine Ammonium Oxidizer Under Energy-Source Deprivation. *Mar. Ecol.* **1985**, *26*, 175–179. [CrossRef]
19. Johnstone, B.H.; Jones, R.D. Recovery of a Marine Chemolithotrophic Ammonium-Oxidizing Bacterium from Long-Term Energy-Source Deprivation. *Can. J. Microbiol.* **1988**, *34*, 1347–1350. [CrossRef]
20. Johnstone, B.; Jones, R. Physiological Effects of Long-Term Energy-Source Deprivation on the Survival of a Marine Chemolithotrophic Ammonium-Oxidizing Bacterium. *Mar. Ecol. Prog. Ser.* **1988**, *49*, 295–303. [CrossRef]
21. Bollmann, A.; Laanbroek, H.J. Continuous Culture Enrichments of Ammonia-Oxidizing Bacteria at Low Ammonium Concentrations. *FEMS Microbiol. Ecol.* **2001**, *37*, 211–221. [CrossRef]
22. Hastings, R.C.; Saunders, J.R.; Hall, G.H.; Pickup, R.W.; McCarthy, A.J. Application of Molecular Biological Techniques to a Seasonal Study of Ammonia Oxidation in a Eutrophic Freshwater Lake. *Appl. Environ. Microbiol.* **1998**, *64*, 3674–3682. [CrossRef]
23. Speksnijder, A.G.C.L.; Kowalchuk, G.A.; Roest, K.; Laanbroek, H.J. Recovery of a Nitrosomonas-like 16S RDNA Sequence Group from Freshwater Habitats. *Syst. Appl. Microbiol.* **1998**, *21*, 321–330. [CrossRef] [PubMed]
24. Abbaszadeh, L.; Koutra, E.; Tsigkou, K.; Gaspari, M.; Kougias, P.G.; Kornaros, M. Nitrification upon Nitrogen Starvation and Recovery: Effect of Stress Period, Substrate Concentration and PH on Ammonia Oxidizers' Performance. *Fermentation* **2022**, *8*, 387. [CrossRef]
25. Gujer, W. Nitrification and Me—A Subjective Review. *Water Res.* **2010**, *44*, 1–19. [CrossRef] [PubMed]
26. Ni, B.-J.; Ruscalleda, M.; Pellicer-Nacher, C.; Smets, B.F. Modeling Nitrous Oxide Production during Biological Nitrogen Removal via Nitrification and Denitrification: Extensions to the General ASM Models. *Environ. Sci. Technol.* **2011**, *45*, 7768–7776. [CrossRef]
27. Rausch, T. The Estimation of Micro-Algal Protein Content and Its Meaning to the Evaluation of Algal Biomass I. Comparison of Methods for Extracting Protein. *Hydrobiologia* **1981**, *78*, 237–251. [CrossRef]
28. Eaton, A.D.; Clesceri, L.S.; Greenberg, A.E.; Franson, M.A.H. *Standard Methods for the Examination of Water and Wastewater*, 22nd ed.; APHA: Washington, DC, USA, 2012.
29. Ostace, G.S.; Cristea, V.M.; Agachi, P.Ş. Extension of Activated Sludge Model No 1 with Two-Step Nitrification and Denitrification Processes for Operation Improvement. *Environ. Eng. Manag. J.* **2011**, *10*, 1529–1544. [CrossRef]
30. Zhang, D.; Cai, Q.; Zu, B.; Bai, C.; Zhang, P. The Influence of Trace NO_2 on the Kinetics of Ammonia Oxidation and the Characteristics of Nitrogen Removal from Wastewater. *Water Sci. Technol.* **2010**, *62*, 1037–1044. [CrossRef] [PubMed]
31. Jiménez, E.; Giménez, J.B.; Ruano, M.V.; Ferrer, J.; Serralta, J. Effect of PH and Nitrite Concentration on Nitrite Oxidation Rate. *Bioresour. Technol.* **2011**, *102*, 8741–8747. [CrossRef]
32. Xie, Y.; Xu, J.; Yang, R.; Alshammari, J.; Zhu, M.-J.; Sablani, S.; Tang, J. Moisture Content of Bacterial Cells Determines Thermal Resistance of Salmonella Enterica Serotype Enteritidis PT 30. *Appl. Environ. Microbiol.* **2021**, *87*, e02194-20. [CrossRef] [PubMed]
33. Tsafrakidou, P.; Manthos, G.; Zagklis, D.; Mema, J.; Kornaros, M. Assessment of Substrate Load and Process PH for Bioethanol Production–Development of a Kinetic Model. *Fuel* **2022**, *313*, 123007. [CrossRef]
34. Rittmann, B.E.; McCarty, P.L. *Environmental Biotechnology: Principles and Applications*; McGraw-Hill Education: New York, NY, USA, 2001; ISBN 1260440591.
35. Liu, X. Comparing Three Mathematical Models Using Different Substrates for Prediction of Partial Nitrification. *Sci. Total Environ.* **2020**, *749*, 141643. [CrossRef] [PubMed]
36. Cui, F.; Park, S.; Mo, K.; Lee, W.; Lee, H.; Kim, M. Experimentation and Mathematical Models for Partial Nitrification in Aerobic Granular Sludge Process. *KSCE J. Civ. Eng.* **2017**, *21*, 127–133. [CrossRef]
37. Thalla, A.K.; Bhargava, R.; Kumar, P. Nitrification Kinetics of Activated Sludge-Biofilm System: A Mathematical Model. *Bioresour. Technol.* **2010**, *101*, 5827–5835. [CrossRef]
38. Prosser, J.I. Autotrophic Nitrification in Bacteria. In *Advances in Microbial Physiology*; Rose, A.H., Tempest, D.W., Eds.; Academic Press: Cambridge, MA, USA, 1990; Volume 30, pp. 125–181, ISBN 0065-2911.